Streptococcus oralis Biofilm Formation on Titanium Surfaces

Simonetta D'Ercole, PhD, DDS[1]/Emanuela Di Campli[2]/Serena Pilato, PhD Student[3]/
Giovanna Iezzi, PhD, DDS[4]/Luigina Cellini[2]/Adriano Piattelli, MD[5]/Morena Petrini, DDS, PhD[4]

Purpose: The aim of this study was to compare the *Streptococcus oralis* biofilm formation on titanium machined turned surfaces and sandblasted surfaces that were previously characterized for their superficial topographies. ***Materials and Methods:*** Two commercially pure titanium surfaces were analyzed and compared: machined (turned surfaces subjected to a process of decontamination that also included a double acid attack) and sandblasted (sandblasted surfaces, cleaned with purified water, enzymatic detergent, acetone, and alcohol). The characterization of the samples at the nanolevel was performed using atomic force microscopy, which permitted calculation of the superficial nanoroughness (Ra). The sessile drop method was used to measure the water contact angle in both groups and allowed information to be gained about their wetting properties. Scanning electron microscope and energy-dispersive x-ray spectroscopy analysis allowed comparison of the microtopographic geometry and the chemical composition of the samples. Then, the disks were pre-incubated with saliva in order to form an acquired pellicle. *Streptococcus oralis* was put on the disks, and both groups were tested at 24 and 48 hours for biofilm biomass evaluation, colony-forming units (CFUs), and live/dead staining for cell viability. ***Results:*** The sandblasted samples were characterized by a significantly higher level of superficial oxides, superficial roughness, and hydrophilicity, compared with the machined turned samples. Although there were topographic differences, the *Streptococcus oralis* biofilm formation, quantified in CFUs, and biomass formation at 24 and 48 hours were similar in both groups. With the live/dead staining, the sandblasted disks were characterized by an increased percentage of dead cells compared with the machined disks. ***Conclusion:*** Although significant topographic differences were present between machined and sandblasted disks, the *Streptococcus oralis* biofilm formation seems to not be significantly affected. *Int J Oral Maxillofac Implants 2021;36:929–936. doi: 10.11607/jomi.8739*

Keywords: bacteria, biofilm, biomaterials, microbiology, nanosurfaces, titanium surface

The aim of research in implant dentistry is to produce surfaces that promote osseointegration but also have an antibacterial effect in order to counteract the risk of peri-implantitis.[1,2]

[1]Orthodontics, Microbiology and Pediatric Dentistry Unit, Department of Medical, Oral and Biotechnological Sciences, University of Chieti, Chieti, Italy.
[2]Microbiology Unit, Department of Pharmacy, University of Chieti, Chieti, Italy.
[3]Department of Pharmacy, University of Chieti, Chieti, Italy.
[4]Department of Medical, Oral and Biotechnological Sciences, University of Chieti-Pescara, Chieti Scalo, CH, Italy.
[5]Department of Medical, Oral and Biotechnological Sciences, University "G. d'Annunzio" Chieti-Pescara, Italy; University of Valencia, Valencia, Spain (Laurea Honoris Causa); Catholic University of San Antonio de Murcia (UCAM), Murcia, Spain (Laurea Honoris Causa); Fondazione Villa Serena per la Ricerca, Città S. Angelo (PE), Italy; Casa di Cura Villa Serena del dott. L. Petruzzi, Città S. Angelo (PE), Italy.

Correspondence to: Dr Morena Petrini, Junior Researcher, Department of Medical, Oral and Biotechnological Sciences, University of Chieti, Via Vestini 31, 66013 Chieti, Italy.
Email: petrini.morena@gmail.com or morena.petrini@unich.it

Submitted June 15, 2020; accepted May 15, 2021.

In particular, the properties of the surface and biochemical, mechanical, and topographic layers are able to interact with cells and influence their adhesion, diffusion, migration, proliferation, and differentiation.[3]

The presence of topographic features on titanium surfaces, at the microlevel, are able to influence, in the first phases after the implant insertion, both the neo-osteogenesis and the removal torque; however, the angiogenesis seems to be more affected by the nanotopography and chemical surfaces of the implants.[4–6]

In particular, only the superficial features comprised between 70 nm and 5 mm, independently from the shape, seem to effectively interact with cells by means of membrane alterations.[3,7] Recently, investigations at the nanoscale level (1 to 100 nm) have increased in popularity, thanks to the introduction of novel technologies, which showed their impact on increasing the bone-to-implant contact and, consequently, also the protein adsorption on biomaterials and the cell interactions.[8,9]

The wettability of a material is influenced by both the superficial roughness and the chemical properties.[10] In particular, an increase in the surface roughness (Ra) leads to a reduction of the angle of contact with water in hydrophilic surfaces but has an opposite effect on hydrophobic surfaces.[11,12]

However, a superficial treatment could increase the host stem cells to adhere, proliferate, mature, and differentiate,[13] but at the same time, it could improve bacterial adhesion, creating the conditions for the etiology of pathologies such as peri-implantitis.[14]

Indeed, just as the subgingival microflora associated with periodontitis stabilizes around natural teeth, dental implants soon become contaminated immediately after the insertion.[15] The biofilm formation on the implant surface and an excessive host response seem to have an important role in the initiation and progression of peri-implantitis.[16] Peri-implantitis is a complex inflammatory disease that causes the loss of bone supporting the implant, and as with periodontitis, it has been mainly associated with a gram-negative, anaerobic type of bacteria, such as *Porphyromonas gingivalis*.[17] This periodonto-pathogen bacterium has also been linked with more serious systemic diseases, such as diabetes, hypertension, and Alzheimer's disease.[18,19]

Also, opportunistic pathogens such as *S aureus*, *P aeruginosa*, and *C albicans* may be associated with implant failure.[17,20,21] However, gram-positive microorganisms, such as *Streptococcus oralis*, are the first colonizers of the implant surfaces, above which more pathogenic species involved in the pathogenesis of the peri-implant disease aggregate.

The objective of this study was to explore the influence of two different superficial topographies of titanium disks, machined turned and sandblasted, on *Streptococcus oralis* biofilm formation.

MATERIALS AND METHODS

Titanium Surfaces

The materials and methods were in accordance with the EQUATOR guidelines, standards for reporting qualitative research: a synthesis of recommendations (SRQR).[22]

A total of 150 commercially pure Titanium ASTM f67 (Implacil De Bortoli) were used as substrate material in this study. The disks were 5 mm in diameter and 2 mm in thickness. In particular, two different groups of 75 disks each and characterized by two different surfaces were analyzed and compared:

- Machined: turned surfaces cleaned with purified water, enzymatic detergent, acetone, acetylic acid (double acid attack), and alcohol
- Sandblasted: sandblasted surfaces (turned surfaces sanded with a mix of TiO_2 powders) cleaned with purified water, enzymatic detergent, acetone, and alcohol

The following controls were also analyzed to verify the correctness of the microbiologic assays:

- C–: negative controls—new disks without bacteria inoculation
- C+: positive controls—bacterium inoculated on polystyrene surface

All samples were placed for 60 minutes in 75% ethanol, and after drying, they were irradiated for 30 minutes with ultraviolet (UV) light. Then, they were put in 96-well polystyrene microtiter plates for 2 hours in saliva incubation, with slight agitation, to permit the formation of the acquired pellicle.[1,2]

Atomic Force Microscopy

Atomic force microscopy (AFM; Bruker) with a RTESPA-300 probe (Bruker) was used to study the superficial nanotopography and then to calculate the nanoroughness average (Ra) of the surfaces.

In particular, the following parameters were adopted for the AFM observation: ScanAsyst technique (Bruker), with a scan size of 10 µm. The Nanoscope software (Bruker) was employed for the image analysis and the 3D reconstruction. In particular, the arithmetic mean of the absolute values of the height of the surface profile, the average roughness (Ra), was calculated in three different samples of each group and was reported as mean values (± SD).

Scanning Electron Microscope Observation and Energy-Dispersive X-ray Spectroscopy

A scanning electron microscope (SEM; Phenom ProX, Phenom-World BV) in association with specific software, Element Identification (Phenom-World BV), was employed for samples at microscale, and energy-dispersive x-ray spectroscopy (EDS) analysis was run, with the following field of view (FOV) parameters: 559 µm, Mode: 15 kV - Map, detector: full BSD. Three disks were observed for each group.

Measurement of the Wetting Properties

The sessile drop method was used to measure the wetting properties of the groups, as previously described.[11] The water contact angle and the wetted area were measured using ImageJ 1.52q for Mac OS X (Apple), Fig 1. Three samples of each group were observed, and the sandblasted disks were compared with the control disks. The percentage of increase of the wetted area was calculated in respect to the control disks.

Microbial Strain

A clinical strain of *Streptococcus oralis* CH 05, isolated by saliva samples from one healthy patient, and stored at –80°C, was used for this study.[23] Reconstitution overnight at 37°C under anaerobic condition in Brain Heart Infusion broth (BHI, Oxoid) was followed by a 1:10 dilution in the same medium and later was refreshed

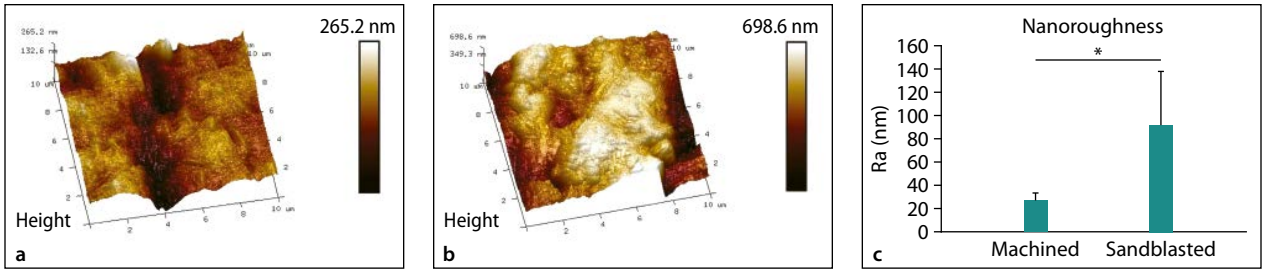

Fig 1 3D reconstruction of AFM images of *(a)* machined and *(b)* sandblasted surfaces with *(c)* the relative graph of the average Ra. Error bars = SD.

for 2 hours at 37°C in a shaking thermostatic water bath (160 rpm). For the experiment, a suspension was used containing 9×10^6 CFU/mL bacteria, which was obtained by diluting the solution until reaching the optical density OD_{600} = 0.12, verified by the spectrophotometer (Eppendorf).

Saliva Collection

Saliva was obtained from four volunteers, who were systemically healthy, with the spitting method, as previously described.[24,25] The use of human saliva was approved by the Local Ethical Committee.

Saliva samples were mixed, centrifuged at 16,000× g for 1 hour at 4°C, and passed consecutively through low protein binding filters (pore sizes of 0.8, 0.45, and 0.2 µm).[26]

To test the sterility of the saliva, 1-mL aliquots of samples were plated on Tryptic Soy Agar (TSA, Becton Dickinson) and incubated in both aerobic and anaerobic atmosphere for 24 to 48 hours at 37°C. Saliva that showed no growth was considered sterile and then stored at –20°C for a maximum of 2 days.[27]

Biofilm Development

Two hundred µL of *Streptococcus oralis* CH 05 bacterial suspension was added on the disks coated with saliva and left to incubate at 37°C for 24 hours and 48 hours under anerobic condition.

Then, microbial suspensions and any nonadherent bacteria were removed by washing the samples three times with phosphate-buffered saline (PBS).

Each microbiologic experiment was conducted three times on each type of disk after 24 and 48 hours of incubation, so a total of 66 disks for each group were used.

Determination of Colony-Forming Units (CFUs)

After washing with PBS, the disks were placed in sterile test tubes containing 1 mL PBS. Nonadherent bacteria were removed from titanium disks by putting them into the water of a 40-kHz ultrasonic cleaning bath for 4 minutes (Euronda) and then vortexing for 2 minutes. Prior to plating, the microbial suspension, through live/dead staining, was observed by microscopy that confirmed the presence of a mixture of single, viable microbial cells (data not shown).

Then, selected 10-fold dilutions were plated on TSA-agar plates and incubated overnight at 37°C, followed by counting of CFU/mL. The number of adhesive bacteria on the surface of the specimen was calculated.

Biofilm Biomass Assay

The biomass assay measured both the bacterial cells and the presence of extracellular polymeric substances at 24 and 48 hours of bacterial inoculation. Then, the samples were washed three times with PBS, fixed by air drying, stained with Crystal Violet 0.1% (Sigma Aldrich) for 1 minute, washed with PBS, and eluted with ethanol for reading. After 10 minutes, the biomass was quantified as the absorbance at 570 nm of the samples measured with a microplate reader (SAFAS).

Cell Viability Assay

For the evaluation of cell viability, the biofilm growth on the disks was examined with a BacLight LIVE/DEAD Viability Kit (Molecular Probes, Invitrogen Detection Technologies). After the removal of planktonic bacteria by aspiration and the washing of the disks with PBS, the samples were stained for 15 minutes in the dark with SYTO 9 to highlight the viable cells in green and with propidium iodide to stain those with impaired membrane activity in red. The images visualized under a fluorescent Leica 4000 DM microscope (Leica Microsystems) equipped with a halogen lamp, Neoplan 100/1.25 oil objective, and 1713 filter cube (fluorescein; 490/510/520 nm), were recorded at an emission wavelength of 500 nm for SYTO 9 and at 635 nm for propidium iodide.[28] The enumeration was performed by three blinded microbiologists (S.D.E., E.D.C., L.C.) by using image analysis software (LEICA QWin) through the examination of at least 10 random fields of each view, as previously shown.[11,23,29,30]

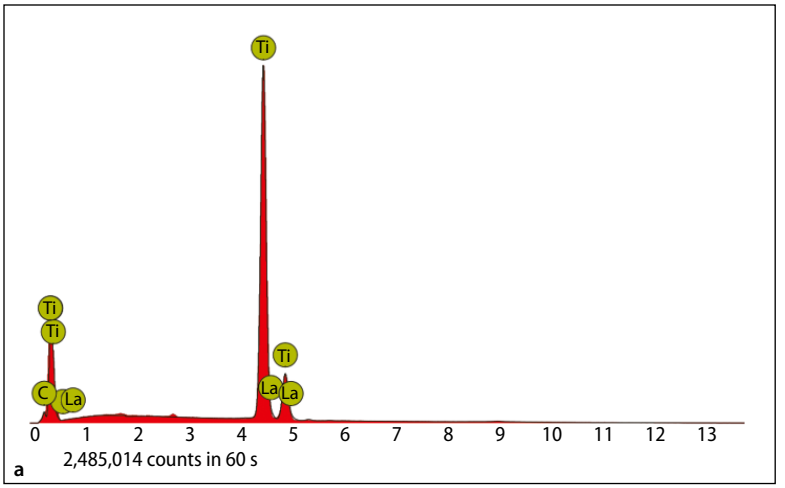

a

Element symbol	Atomic concentration	Weight concentration	Oxide symbol	Stoichiometric weight concentration
Ti	97.07	94.89	TiO_2	96.38
La	1.69	4.81	La_2O_3	3.43
C	1.24	0.30		

b

Fig 2 The superficial chemical composition of machined disks at EDS analysis with the *(a)* relative graph and *(b)* table. *(c)* The SEM observation of the sample analyzed by EDS.

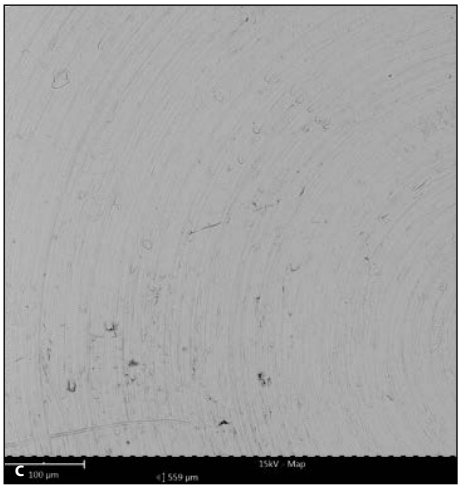

c

Statistical Analysis

The software for statistical analysis SPSS 21 (IBM SPSS) was used to calculate analysis of variance (ANOVA) and the *t* test for independent variables and to evaluate the significant differences at intragroup and intergroup analysis. CFUs were expressed as log10CFUs.

P values < .05 were considered significant.

RESULTS

The AFM observations showed that the sandblasted group was characterized by a significantly higher Ra of 91.800 ± 48.144 nm, compared with the Ra of the machined group, 26.800 ± 6.422 nm ($P = .015$), as shown in Fig 2. The high standard deviation of the sandblasted group confirms the high heterogeneity of the surfaces that is possible to observe in Fig 1b. The EDS analysis confirmed that the machined disks (Figs 1a and 1b) were composed mainly of titanium and some traces of lanthanum (La) and carbonium (C). The SEM observation (Fig 1c) showed the very regular structure of this surface, which was characterized by the presence of circumferential and parallel lines.

The percentage of oxygen significantly increased on sandblasted disks, reaching 24.71% of the weight concentration (Figs 3a and 3b); also, 4.07% aluminum (Al) was recorded. The microtopographic features of this group observed at SEM (Fig 3c) revealed a very rough and heterogenous surface, characterized by the random disposition of irregular asperities and concavities.

The study of the wetting properties of the samples, Fig 4, showed that sandblasted samples were characterized by a significantly higher hydrophilicity, as confirmed by the significant decrease of the water contact angle (Figs 4a and 4b) and the increase of the wetted area (Figs 4c and 4d).

On the contrary, the microbiologic analysis of *S oralis* biofilm showed that there were no significant differences, both at the intragroup and intergroup analysis, concerning the CFUs (Fig 5a) and the biomass (Fig 5b) after 24 and 48 hours of incubation.

These data were also confirmed by the live/dead staining that did not show significant differences among the samples, although the percentage of death cells were higher in the sandblasted disks at 24 hours compared with the machined disks, but at 48 hours, both groups had similar percentages (Fig 6). Biomass in sandblasted disks was characterized by a similar trend compared with the machined disks.

At 48 hours, it was possible to observe an increase of biofilm organization in both groups.

DISCUSSION

In this in vitro study, titanium disks with different surfaces were characterized and then incubated with saliva in order to permit *S oralis* to interact with an

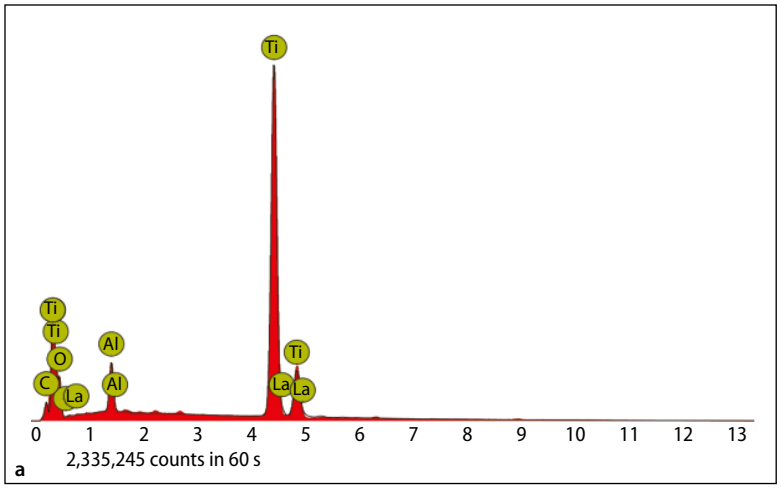

Element symbol	Atomic concentration	Weight concentration	Oxide symbol	Stoichiometric weight concentration
O	48.90	24.71		
Ti	44.48	67.26	TiO_2	90.14
Al	4.78	4.07	Al_2O_3	6.18
C	1.03	0.39		
La	0.81	3.57	La_2O_3	3.36

b

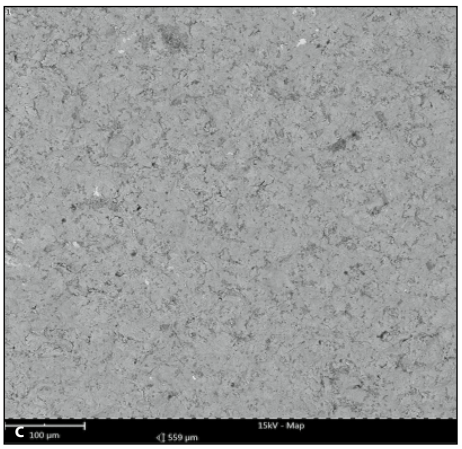

Fig 3 The superficial chemical composition of sandblasted disks at EDS analysis with the *(a)* relative graph and *(b)* table. *(c)* The SEM observation of the sample analyzed by EDS.

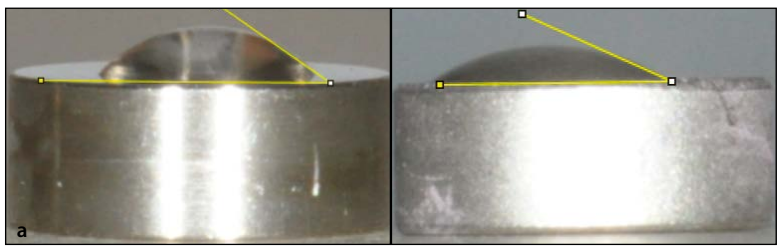

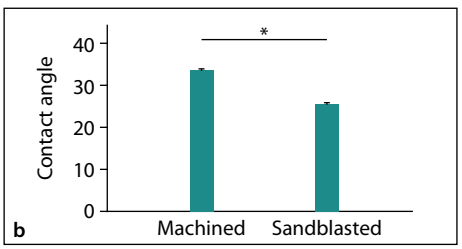

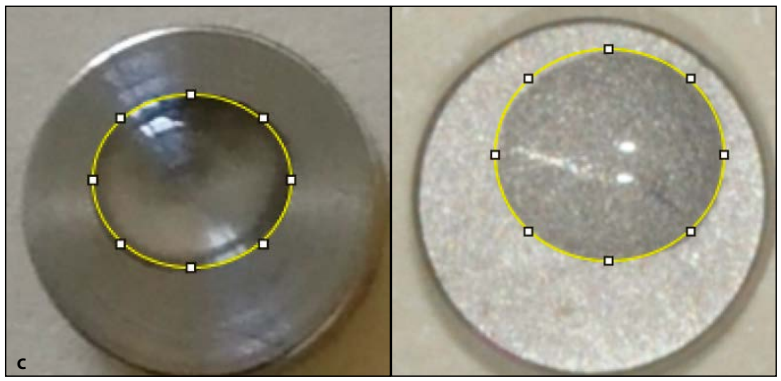

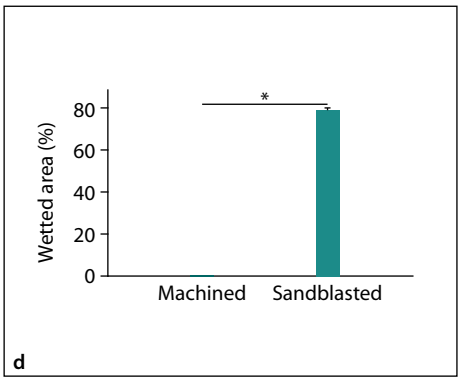

Fig 4 *(a)* Images and *(b)* relative graphs of water contact angle of machined *(left)* and sandblasted *(right)* surfaces. *(c)* Images of the wetted area of the samples. *(d)* Percentage of increase of wetted area of sandblasted vs machined. Error bars = ± SD. *$P < .05$.

acquired pellicle, like in vivo conditions. This bacterium is considered one of the first pioneers that permit the co-adherence of later colonizers, leading to the formation of mature oral biofilms.[31] Investigations of the interactions between bacterial pioneers and biomaterials are fundamental for preventing prosthetic failures, and in particular, emerging evidence shows the important interconnection between titanium surfaces, oral biofilm, and the innate immune system, for the development of peri-implantitis.[16,32,33] The battle against

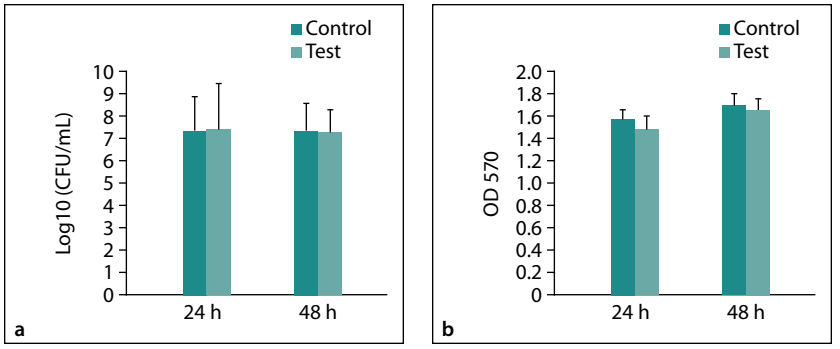

Fig 5 Colony-forming units expressed in *(a)* Log10 (CFUs/mL) and *(b)* biomass of adherent *S oralis* on machined and sandblasted disks at 24 and 48 hours (error bars = ± SD).

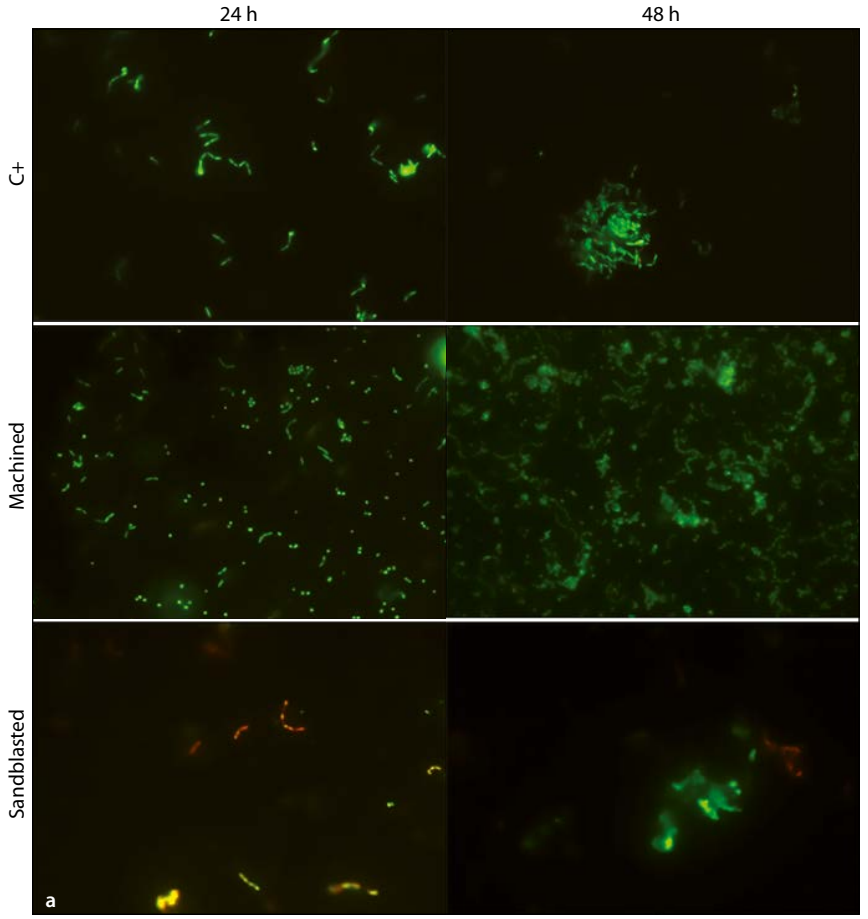

Fig 6 Representative images of live/dead stainings. Results were compared with positive controls (C+), which were bacteria inoculated on polystyrene surfaces (*$P < .05$).

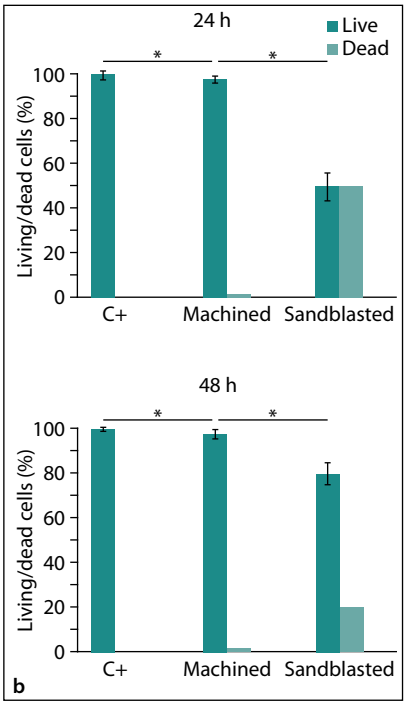

peri-implantitis represents a challenge for both researchers and clinicians in finding an efficient protocol or alternative modalities of treatment that could permit eradication of this disease.[34–41] Indeed, a recent survey showed that although there is an increasing trend in using dental implants in the population, at least 11% of the patients reported long-term complications, which in 82% were of biologic origin, and in 46% of these, it was necessary to remove the implants.[42]

This work showed that, although the nanoroughness and hydrophilicity of sandblasted surfaces are higher, no significant differences compared with machined surfaces were found concerning the biofilm formation. These results are in accordance with other in vitro studies that showed that early bacterial colonization of titanium surfaces was not significantly influenced by the superficial roughness.[15,43]

The results of this work are in line with other studies that showed that roughness increases the bacterial adhesion only in the first minutes, but then, after the biofilm formation, these differences decrease and are nullified after the 15th hour.[44] Another study by Di Giulio et al found a higher level of *P gingivalis* on machined turned titanium disks compared with the treated ones.[11]

In this study, no significant differences were found between sandblasted and machined surfaces for CFUs and biomass at 24 and 48 hours, but live/dead images showed significant differences in the ratio between live and dead cells in the two groups at 24 hours. In particular, sandblasted surfaces were characterized by a higher percentage of dead cells.

EDS analysis showed a significantly higher level of superficial oxides in sandblasted samples compared with machined samples. This element is very important because titanium dioxide is characterized by photocatalytic activity, and when exposed to UVs, produces reactive oxygen species that inactivate bacteria, viruses, and fungi.[45] Thus, the antibacterial effect exerted by the superficial chemical composition of sandblasted samples could have counterbalanced the higher pro-adhesive characteristics of higher roughness and hydrophilicity compared with machined samples. The clinical implications of this study are very encouraging because of the treated surfaces, although the better interaction with the bone and the lower early failure rates are not associated with increased biofilm formation in the first 48 hours.

CONCLUSIONS

The microbiologic analysis showed no significant differences between sandblasted and machined disks, although the superficial topographies showed by the two groups were significantly different.

ACKNOWLEDGMENTS

This work was supported by the Adriano Piattelli ex 60% University of Chieti–Pescara Fund, and partly by the Progetti di Ricerca di Rilevante Interesse Nazionale, grant number 20102ZLNJ5, financed by the Ministry of Education, University, and Research (MIUR), Rome, Italy. The authors reported no conflicts of interest related to this study.

REFERENCES

1. D'Ercole S, Cellini L, Pilato S, et al. Material characterization and Streptococcus oralis adhesion on Polyetheretherketone (PEEK) and titanium surfaces used in implantology. J Mater Sci Mater Med 2020;31:84.
2. Petrini M, Giuliani A, Di Campli E, et al. The bacterial anti-adhesive activity of double-etched titanium (DAE) as a dental implant surface. Int J Mol Sci 2020;21:8315.
3. Ventre M, Causa F, Netti PA. Determinants of cell-material crosstalk at the interface: Towards engineering of cell instructive materials. J R Soc Interface 2012;9:2017–2032.
4. Cordioli G, Majzoub Z, Piattelli A, Scarano A. Removal torque and histomorphometric investigation of 4 different titanium surfaces: An experimental study in the rabbit tibia. Int J Oral Maxillofac Implants 2000;15:668–674.
5. Scarano A, Degidi M, Perrotti V, Degidi D, Piattelli A, Iezzi G. Experimental evaluation in rabbits of the effects of thread concavities in bone formation with different titanium implant surfaces. Clin Implant Dent Relat Res 2014;16:572–581.
6. Saghiri MA, Asatourian A, Garcia-Godoy F, Sheibani N. The role of angiogenesis in implant dentistry part I: Review of titanium alloys, surface characteristics and treatments. Med Oral Patol Oral Cir Bucal 2016;21:e514–e525.
7. Lamers E, van Horssen R, te Riet J, et al. The influence of nanoscale topographical cues on initial osteoblast morphology and migration. Eur Cell Mater 2010;20:329–343.
8. Simchi A, Tamjid E, Pishbin F, Boccaccini AR. Recent progress in inorganic and composite coatings with bactericidal capability for orthopaedic applications. Nanomedicine 2011;7:22–39.
9. Kulkarni M, Patil-Sen Y, Junkar I, Kulkarni CV, Lorenzetti M, Iglič A. Wettability studies of topologically distinct titanium surfaces. Colloids Surf B Biointerfaces 2015;129:47–53.
10. Marmur A. A guide to the equilibrium contact angles maze. In: Mittal KL. Contact Angle, Wettability and Adhesion, Volume 6. London: CRC Press, 2009.
11. Di Giulio M, Traini T, Sinjari B, Nostro A, Caputi S, Cellini L. Porphyromonas gingivalis biofilm formation in different titanium surfaces, an in vitro study. Clin Oral Implants Res 2016;27:918–925.
12. Riveiro A, Maçon ALB, del Val J, Comesaña R, Pou J. Laser surface texturing of polymers for biomedical applications. Front Phys 2018;6.
13. Damiati L, Eales MG, Nobbs AH, et al. Impact of surface topography and coating on osteogenesis and bacterial attachment on titanium implants. J Tissue Eng 2018;9:2041731418790694.
14. Quirynen M, van der Mei HC, Bollen CM, et al. An in vivo study of the influence of the surface roughness of implants on the microbiology of supra- and subgingival plaque. J Dent Res 1993;72:1304–1309.
15. Schmidlin PR, Müller P, Attin T, Wieland M, Hofer D, Guggenheim B. Polyspecies biofilm formation on implant surfaces with different surface characteristics. J Appl Oral Sci 2013;21:48–55.
16. Daubert DM, Weinstein BF. Biofilm as a risk factor in implant treatment. Periodontol 2000 2019;81:29–40.
17. Albertini M, López-Cerero L, O'Sullivan MG, et al. Assessment of periodontal and opportunistic flora in patients with peri-implantitis. Clin Oral Implants Res 2015;26:937–941.
18. Graziani F, Gennai S, Solini A, Petrini M. A systematic review and meta-analysis of epidemiologic observational evidence on the effect of periodontitis on diabetes: An update of the EFP-AAP review. J Clin Periodontol 2018:167–187.
19. Solini A, Suvan J, Santini E, et al. Periodontitis affects glucoregulatory hormones in severely obese individuals. Int J Obes (Lond) 2019;43:1125–1129.
20. Petrini M, Trentini P, Tripodi D, Spoto G, D'Ercole S. In vitro antimicrobial activity of LED irradiation on Pseudomonas aeruginosa. J Photochem Photobiol B Biol 2017;168:25–29.
21. Ardila CM, Ramón-Morales OM, Ramón-Morales CA. Opportunistic pathogens are associated with deteriorated clinical parameters in peri-implant disease. Oral Dis 2020 Apr 5. [Epub ahead of print]
22. O'Brien BC, Harris IB, Beckman TJ, Reed DA, Cook DA. Standards for reporting qualitative research: A synthesis of recommendations. Acad Med 2014;89:1245–1251.
23. D'Ercole S, Di Giulio M, Grande R, et al. Effect of 2-hydroxyethyl methacrylate on Streptococcus spp. biofilms. Lett Appl Microbiol 2011;52:193–200.
24. Petrini M, Costacurta M, Ferrante M, Trentini P, Docimo R, Spoto G. Association between the organoleptic scores, oral condition and salivary β-galactosidases in children affected by halitosis. Int J Dent Hyg 2014;12:213–218.
25. Petrini M, Trentini P, Ferrante M, D'Alessandro L, Spoto G. Spectrophotometric assessment of salivary β-galactosidases in halitosis. J Breath Res 2012;6:021001.
26. Di Giulio M, di Giacomo V, Di Campli E, et al. Saliva improves Streptococcus mitis protective effect on human gingival fibroblasts in presence of 2-hydroxyethyl-methacrylate. J Mater Sci Mater Med 2013;24:1977–1983.
27. Di Giulio M, Di Valerio V, Bosco D, et al. Molecular mechanisms driving Streptococcus mitis entry into human gingival fibroblasts in presence of chitlac-nAg and saliva. J Mater Sci Mater Med 2018;29:36.
28. Petrini M, Spoto G, Scarano A, et al. Near-infrared LEDS provide persistent and increasing protection against E. faecalis. J Photochem Photobiol B Biol 2019;197:111527.
29. Cataldi A, Gallorini M, Di Giulio M, et al. Adhesion of human gingival fibroblasts/Streptococcus mitis co-culture on the nanocomposite system Chitlac-nAg. J Mater Sci Mater Med 2016;27:88.

30. Hahnel S, Wieser A, Lang R, Rosentritt M. Biofilm formation on the surface of modern implant abutment materials. Clin Oral Implants Res 2015;26:1297–1301.
31. Kolenbrander PE, Palmer RJ Jr, Periasamy S, Jakubovics NS. Oral multispecies biofilm development and the key role of cell-cell distance. Nat Rev Microbiol 2010;8:471–480.
32. Albrektsson T, Dahlin C, Reinedahl D, Tengvall P, Trindade R, Wennerberg A. An imbalance of the immune system instead of a disease behind marginal bone loss around oral implants: Position paper. Int J Oral Maxillofac Implants 2020;35:495–502.
33. Yu F, Addison O, Baker SJ, Davenport AJ. Lipopolysaccharide inhibits or accelerates biomedical titanium corrosion depending on environmental acidity. Int J Oral Sci 2015;7:179–186.
34. Fernandes-Costa AN, Menezes KM, Borges SB, Roncalli AG, Calderon PDS, de V Gurgel BC. A prospective study of the clinical outcomes of peri-implant tissues in patients treated for peri-implant mucositis and followed up for 54 months. Clin Implant Dent Relat Res 2019;21:1099–1105.
35. D'Ercole S, Spoto G, Trentini P, Tripodi D, Petrini M. In vitro inactivation of Enterococcus faecalis with a led device. J Photochem Photobiol B 2016;160:172–177.
36. Petrini M, Spoto G, Scarano A, et al. Near-infrared LEDS provide persistent and increasing protection against E. faecalis. J Photochem Photobiol B 2019;197:111527.
37. Alhaidary D, Franzen R, Hilgers RD, Gutknecht N. First investigation of dual-wavelength lasers (2780 nm Er,Cr:YSGG and 940 nm Diode) on implants in a simulating peri-implantitis situation regarding temperature changes in an in vitro pocket model. Photobiomodul Photomed Laser Surg 2019;37:508–514.
38. Caplanis N, Kusek ER, Low S, Linden E, Sporborg H. Peri-implantitis, a consensus for treatment: A case study. J Oral Implantol 2019;45:371–377.
39. Radunović M, Petrini M, Vlajic T, et al. Effects of a novel gel containing 5-aminolevulinic acid and red LED against bacteria involved in peri-implantitis and other oral infections. J Photochem Photobiol B 2020;205:111826.
40. Rahman SU, Mosca RC, Govindool Reddy S, et al. Learning from clinical phenotypes: Low-dose biophotonics therapies in oral diseases. Oral Dis 2018;24:261–276.
41. Scarano A, Lorusso F, Inchingolo F, Postiglione F, Petrini M. The effects of Erbium-doped Yttrium aluminum garnet laser (Er: YAG) irradiation on sandblasted and acid-etched (SLA) titanium, an in vitro study. Materials (Basel) 2020;13:4174.
42. Cairo F, Landi L, Gatti C, Rasperini G, Aimetti M; SIdP, the Italian Society of Periodontology and Implantology. Tooth loss and dental implant outcomes—Where is dentistry going? A survey by SIdP, the Italian Society of Periodontology and Implantology. Oral Dis 2018;24:1379–1381.
43. Pita PP, Rodrigues JA, Ota-Tsuzuki C, et al. Oral streptococci biofilm formation on different implant surface topographies. Biomed Res Int 2015;2015:159625.
44. Fröjd V, Chávez de Paz L, Andersson M, Wennerberg A, Davies JR, Svensäter G. In situ analysis of multispecies biofilm formation on customized titanium surfaces. Mol Oral Microbiol 2011;26:241–252.
45. Arango-Santander S, Pelaez-Vargas A, Freitas SC, García C. A novel approach to create an antibacterial surface using titanium dioxide and a combination of dip-pen nanolithography and soft lithography. Sci Rep 2018;8:15818.